applied optics

Energetic material response to ultrafast indirect laser heating

N. C. Dang,* J. L. Gottfried, and F. C. De Lucia, Jr.

U.S. Army Research Laboratory, 4600 Deer Creek Loop, Aberdeen Proving Ground, Maryland 21005, USA
*Corresponding author: nhan.c.dang.civ@mail.mil

Received 1 August 2016; revised 3 October 2016; accepted 3 October 2016; posted 4 October 2016 (Doc. ID 272989); published 31 October 2016

The initial evolution of thermal energy transfer into a solid explosive is studied using an indirect femtosecond laser heating technique on a picosecond timescale in order to elucidate the role of temperature in the shock-induced initiation of explosives. The indirect laser heating method is presented; time-resolved visible transient absorption (TA) spectroscopy was used to monitor the energetic material response following heat transfer from the laser-heated gold (Au) layer to the sample. Reported here are visible TA data in the spectral region from 500 to 750 nm for indirect laser-heated thin films of cyclotrimethylene trinitramine (RDX), oxidized polyethylene (OPE), and RDX with 1%, 2.5%, 5%, or 10% OPE prior to decomposition. TA was observed for RDX and RDX with OPE; however, no TA was observed for pure OPE. Compared to pure RDX, the TA intensity of RDX with OPE decreases as the OPE content increases and the time required to observe the TA signal from RDX increases. Our results suggest that the thermal energy produced by a femtosecond laser pulse with an energy of 15 mJ cm^{-2} is sufficient to induce changes in the electronic structure of RDX, resulting in promotion of the RDX molecules into an excited state. We also determined that the heat transfer rate in RDX depends on its homogeneity and degree of purity.

OCIS codes: (140.7090) Ultrafast lasers; (300.6530) Spectroscopy, ultrafast; (300.6500) Spectroscopy, time-resolved; (300.1030) Absorption; (300.6550) Spectroscopy, visible; (300.6240) Spectroscopy, coherent transient.

http://dx.doi.org/10.1364/AO.56.000B85

1. INTRODUCTION

Understanding the initial events that occur upon explosive initiation is crucial for determining the sensitivity of explosives and for the control and design of new high explosives. However, the initial events of initiation occur on the picosecond to nanosecond time-scale—and with such a brief transition time, the dynamic response of materials to this perturbation can be very difficult to observe and understand [1–3]. Although there are experiments sensitive to the time- and length-scales necessary to observe the subsequent dynamic response of these materials [4–18], the dynamic shock conditions (pressure, temperature, and strain rate) can all be convolved into the material response, complicating studies of the importance and role of each factor.

Temperature change is thought to play an important role in explosive initiation since it occurs before and during the chemistry it drives. Several competing hypotheses have been proposed regarding the shock-induced initiation mechanisms [19–22]. Among these hypotheses, the role temperature plays in the initiation is discussed. Proposals of "hot spot" formations under external stimuli, such as impact, friction, and shock, leading to ignition of explosives [19,23] suggest that the initiation appears to be thermal in origin. Despite these hypotheses, on the molecular level, very little experimental evidence is available demonstrating how and how fast thermal energy couples into explosive molecules on the characteristic time- and length-scales, or measuring the temperature that drives the initiation. Therefore, observation of the dynamic flow of thermal energy on the timescale of picoseconds is needed to confirm the proposed hypotheses.

Since electronic excitations can be observed on femtosecond time-scales, and vibrational excitations can be observed on hundreds of femtosecond to picosecond time-scales, transient spectroscopies coupled with indirect femtosecond laser heating are the ideal experimental tools to observe these processes. Moreover, femtosecond laser pulse heating significantly enhances the energy density compared to other heating methods, and produces extremely high rates of temperature change (T-jump). For example, assuming total absorption, a 1 fs laser pulse of 1 μJ deposits an energy density that is 10^9 times larger than that which a 1 W continuous wave laser deposits per femtosecond. For a 500 μm thick $CaCO_3$ sample heated with a 10 μJ, 210 fs, 400 nm laser pulse, the rate of T-jump was determined to be $\sim 10^{13}$ K/s [4]. Under extreme high energy densities and

instantaneous temperature jumps, heat conduction behaves in a non-Fourier manner. As discussed in Ref. [24], using the relaxation model for heat conduction in a non-Fourier regime, Maurer and Thompson predicted that, for an instantaneous heat flux of 10^7 W/cm^2, the jump in the temperature may be several hundred degrees in magnitude, resulting in severe thermal stress at the sample surface. Consequently, the molecules in the heated region experience extreme laser heating conditions with a high local density of excited electrons, and the molecular response can vary substantially compared to the response under slower heating conditions. Heating rates during detonation events can reach 10^{10} K/s, with electron densities of the order of 10^7 cm^{-3} [25].

Both theoretical and experimental work has been done to study energy transfer from a flash-heated gold (Au) surface to adsorbed self-assembled monolayers (SAMs) using a flash thermal conductance (indirect flash heating) technique. However, in those studies the focus was on the thermal energy transport across the Au–sample interface; the vibrational transitions of specific SAM functional groups from molecules situated within a few carbon atoms of the Au surface were probed [26–28]. We still need to understand the dynamic processes involved in thermal energy transfer to thicker samples for which the material responses under flash heating closely resemble those in the bulk material. In this work, using the same indirect flash heating technique, we monitored the thermal energy transfer from the Au surface into thin films of cyclotrimethylene trinitramine (RDX) via transient absorption (TA) spectroscopy in experimental conditions under which the RDX did not decompose (i.e., the TA spectra were reproducible at the same sample position).

We further studied the efficiency of thermal energy transfer from the Au surface to thin films of RDX with oxidized polyethylene (OPE), a polymer that is well known for desensitizing the RDX-based polymer binder. The OPE binder was of particular interest to us based on its usage in the plastic-bonded explosive Composition A-3, consisting of 91% RDX [29]. Composition A-3 serves as a model explosive at the U.S. Army Research Laboratory (ARL) for validation of multiscale modeling of energetic material responses to various external stimuli, including heating [30].

2. EXPERIMENTAL

A. Sample Preparation

Military-grade, class 1 RDX was obtained from colleagues at ARL. Neat A-C 656 OPE homo-polymer (CAS 68441-17-8) was obtained from Honeywell and used as received. To prepare mixtures of RDX and OPE, the solid RDX and OPE were first dissolved in acetonitrile and m-xylene, respectively. RDX/OPE mixtures were made by mixing these two solutions such that 1%, 2.5%, 5%, and 10% of OPE by weight in RDX were obtained. Thin films samples were prepared as described in the following steps. A 100 nm thick Au layer was first deposited onto a 0.5 mm thick sapphire substrate using the thermal vapor deposition technique. Then, thin films of RDX or RDX with OPE were prepared by dropping ~30 μL of each solution onto the Au surface. The drop-cast solution was spread out using a spin coater set at 2000 rotations per minute for 90 s.

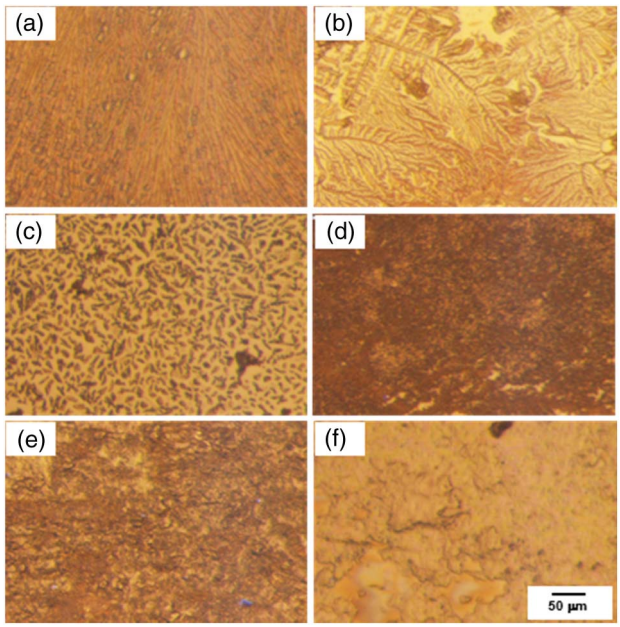

Fig. 1. Micro images of the thin film samples of (a) RDX, (b) RDX with 1% OPE, (c) RDX with 2.5% OPE, (d) RDX with 5% OPE, (e) RDX with 10% OPE, and (f) OPE.

The samples were then allowed to dry in open air at room temperature. The sample thicknesses were determined with a microscope by measuring differences between the focal lengths of the Au surface and the sample surface, and were estimated to be 5.0 (±0.5) μm. The final micro textures of the samples of RDX, OPE, and the RDX with OPE can be seen in Fig. 1. Note that as the OPE content increases, the RDX crystal texture is visibly changed and surrounded more densely with the added OPE.

B. Ultrafast Spectroscopic Method

The femtosecond transient absorption experimental setup is summarized in Fig. 2. In this setup, 1 mJ of a regeneratively

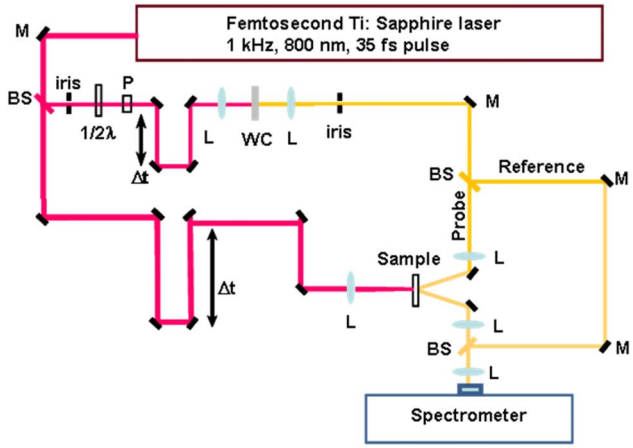

Fig. 2. Schematic diagram of the indirect laser heating with white light transient absorption spectroscopy experiment. M, mirror; BS, beam splitter; L, lens; P, polarizer; $1/2\lambda$, half-wave plate; Δt, time delay translational stage; WC, water cell.

amplified Ti:sapphire laser (Coherent Astrella) with 1 kHz repetition rate, centered at ~800 nm with a pulsewidth of 35 fs was used. An 80:20 beam splitter split the 1 mJ laser beam into two beams. The 80% beam was directed at normal incidence to the back side of the substrate (sapphire–Au surface) through a 125 mm focal lens to produce the heat pump. Upon contact, the laser pulse generated heat on the back surface of the Au layer. The heat then traveled through the Au layer and transferred onto the sample. To prevent ablation of the Au layer or the formation of a laser-induced plasma on the Au surface, the laser energy density was attenuated by adjusting the laser beam size (or adjusting the distance between the sample and the lens) such that the maximum laser energy density resulted in no visible damage to the sapphire–Au interface. Through trial-and-error, we determined that the optimal laser beam diameter (at 120 μJ) was approximately 1 mm, which gives an energy density of the pump at the sapphire–Au interface of ~15 mJ/cm^2.

A small portion of the 20% beam was focused onto a 5 mm thick water cell using a 150 mm focal length lens to generate a white light supercontinuum. To obtain a stable supercontinuum spectrum, the beam size, focal length, and energy of the input 800 nm laser beam was optimized such that nonlinear interactions within the cell were minimal. The supercontinuum was then re-collimated with a 150 mm focal length lens. The beam was further spatially filtered by an iris to obtain the most stable and intense white light spectrum with a beam size ~2 mm in diameter. The supercontinuum was then split into absorption probe and reference beams by a 50:50 beam splitter. The pump and probe beams were spatially and temporally overlapped, and the pump beam was focused on the back side of the sapphire–Au sample substrate, whereas the probe beam was focused on the sample side of the substrate with a spot size of 20 μm. The external angle of incidence on the sample was 30°. The reflected probe and reference pulses were focused with a 75 mm focal length lens onto the 100 μm slit of an imaging spectrometer (custom built). A thermoelectrically cooled, electronically gated CCD detector (Q-imaging Retiga 4000R) recorded the probe and reference intensities simultaneously on each shot with an integration over ~100 pixels after accumulation for each spectral wavelength. The camera pixels were binned 2 × 2 to an effective 1024 pixels in each dimension.

Spectral calibration was performed with atomic emission lamps and optical filters. Timing between the white light supercontinuum and heat pump pulses was determined by pump–probe transient absorption in a 6 μm thick silicon (Si) single crystal. The absorption edge of Si was sufficiently close to the pulse wavelength at 800 nm to allow the 800 nm heat pump to be used as the pump, and the long wavelengths of the supercontinuum were used as the probe. A photodiode with a filter blocking the 800 nm pump scatter monitored the supercontinuum intensity while the time delay between the pump and supercontinuum was scanned. The supercontinuum transmission dropped when the sharply rising initial edge of the pump pulse arrived. The zero time delay (±2 ps) between the supercontinuum and the pump pulse was determined at the initial drop of supercontinuum intensity. During the measurements, the probe intensity spectrum was normalized with respect to the reference for the same laser pulse to account for any fluctuations during measurements. The percentage of transient reflectance under flash heating was first obtained using Eq. (1):

$$R = \left[\frac{R_{\text{pump on}}}{\text{Reference}} - \frac{R_{\text{pump off}}}{\text{Reference}}\right] \Big/ \frac{R_{\text{pump off}}}{\text{Reference}}, \quad \textbf{(1)}$$

where $R_{\text{pump on}}$ and $R_{\text{pump off}}$ are the reflectance during and before heat, respectively. Absorbance was then calculated by

$$A = -\log(R + 1). \quad \textbf{(2)}$$

All spectra were obtained after averaging 100 laser shots in the spectral region from 500 to 750 nm and normalized with the transient absorption spectra of a blank Au surface recorded under identical experimental conditions to correct for Au absorption, which may convolute with the experimentally recorded spectra. Reproducibility of data was checked by performing several runs at the same sample spots as well as at fresh spots. Data were found to be highly consistent.

3. RESULTS AND DISCUSSION

A. Au Surface Transient Absorption

Figure 3(a) shows the 2D time-resolved TA spectra and Fig. 3(b) the absorption intensity profile at 525 nm of an Au surface obtained with a time resolution of 10 ps. The data clearly show that, as discussed in detail in Ref. [31] (and references therein), heat flow in Au occurs predominantly due to two energy carriers, namely, electrons and lattice vibrations, which give rise to an electron temperature and the temperature

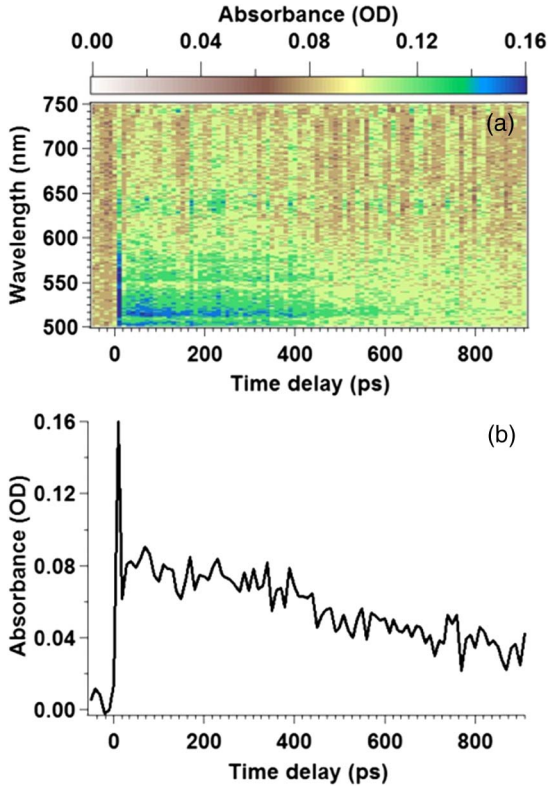

Fig. 3. (a) 2D time-resolved transient absorption spectra and (b) 525 nm absorption intensity profile of a flash heated 100 μm thick Au surface.

at which thermal equilibrium between electrons and the lattice is reached. The sharp T-jump spike produced by electron temperature decays quickly within the first 10 ps, whereas the equilibrium temperature decays slower and lasts for more than 1 ns. Of interest here is the equilibrium temperature since it produces a final heat that sustains long enough for observation of the heat transport in the thin film samples. Therefore, all transient absorption data reported in the following sections were recorded with a time resolution of 50 ps for the purpose of bypassing the electron temperature in the first 10 ps but sufficiently addressing the problems of this study.

B. Transient Absorption of RDX and OPE

Experimentally, TA has been observed in ultrafast laser shock-induced chemistry [14–17]. In those studies, changes in the electronic structure of the excited states were determined to be involved in shock-induced reactions, and redshifted absorption spectra were observed due to formation of new products during reactions. However, questions arose as to whether the changes were caused by shock wave energy or thermal energy from T-jump during the shock loading, or both. If thermal energy contributes to the changes, does it happen before or during the chemical reactions? The primary goal of this study was to look for changes in TA spectra of RDX under indirect laser heating below the RDX decomposition threshold to determine the effect of thermal energy transfer to RDX prior to the onset of irreversible decomposition reactions.

Figure 4 depicts TA spectra due to thermal energy transfer from the Au to the OPE and RDX films as a function of time delay with respect to the heat pump pulse. As seen in Fig. 4(a), no TA was observed for OPE under the experimental conditions of this work. Note that TA records any change in the

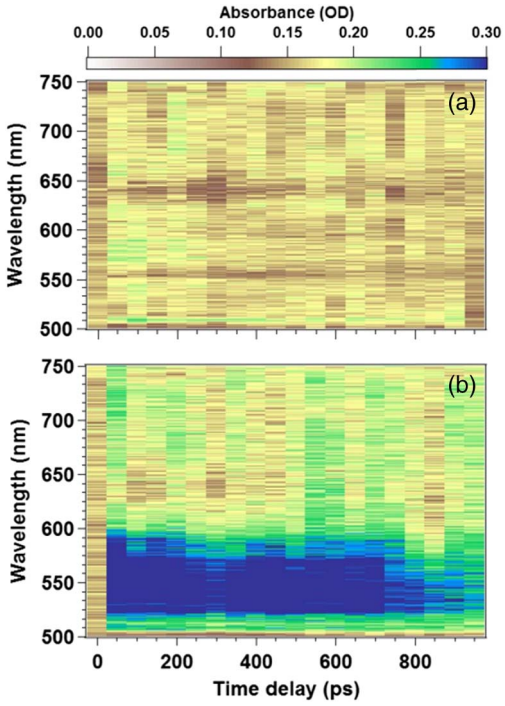

Fig. 4. 2D time-resolved transient absorption spectra of indirect laser heated thin films: (a) OPE and (b) RDX.

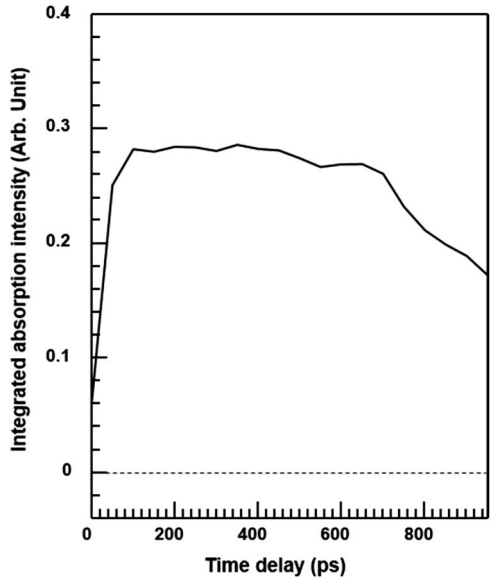

Fig. 5. Time-resolved profile of transient absorption intensity of a thin film RDX illustrating the intensity evolving with time after heating.

absorption spectrum that reflects changes in electronic structures of samples in higher excited states. Therefore, this observation indicates that the provided thermal energy is not high enough to change the electronic structure of OPE molecules and subsequently promote them into the excited state. However, Fig. 4(b) clearly shows that a broad absorption becomes observable in RDX within the first ~50 ps after the heat pump. The absorption reaches a maximum at ~150 ps and levels off after 1 ns, as seen in Fig. 5. These results suggest that the provided thermal energy efficiently alters the electronic structure of the excited RDX to induce absorption in the wavelength region from 500 to 750 nm, and the time required for this energy to thermalize into the sample bath is ~150 ps for the given sample. The above observations for OPE and RDX can be explained by the fact that since the specific heat capacity of OPE ($C_p \sim 2.0$ kJ $\cdot$ K^{-1} $\cdot$ kg^{-1}) is a factor of 2 greater than that found for RDX (C_p of 1.1 kJ $\cdot$ K^{-1} $\cdot$ kg^{-1}), it is expected to require higher heat energy to perturb the electronic structure of OPE compared to that required for RDX.

Examining carefully the spectral features of the TA spectra of indirect laser-heated RDX shown in Fig. 6, no spectral redshift was observed in the TA spectra of the RDX as thermal energy reaches a maximum or the time delay increases. Correlating this observation to the observations in shock-induced reactions for data reported in Refs. [14–17], where spectral redshift was observed at the time and pressure for reactions, it confirms that the changes in the electronic structure of RDX due to thermal energy from the T-jump occurred prior to RDX decomposition. No redshift in the TA suggests that the RDX is unreacted and can be observed before chemical reactions occur (as confirmed by the fact that the TA was reproducible at the same sample location). These results strongly suggest that temperature change is involved in the initial events preceding explosive initiation by changing the electronic structures of the energetic materials.

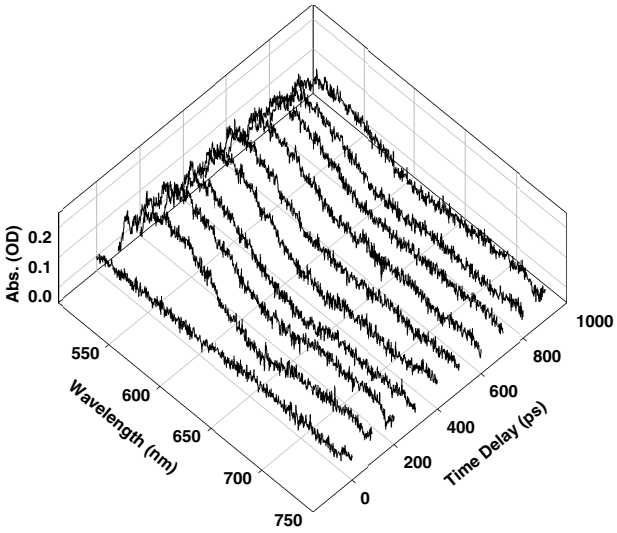

Fig. 6. Transient absorption for indirect laser heated RDX illustrating the spectral changes evolving with time after heating.

From the observation of TA for RDX, a question arose as to whether the temperature raised under these experimental conditions is enough, by itself, to account for promotion of RDX into the excited state. Based on the fact that the melting point temperature of gold is 1337 K and the femtosecond laser energy was selected to avoid damaging the Au layer, the upper bound T-jump (ΔT) of the gold has been estimated to be <800 K [27], which corresponds to an energy increase of at most 0.69 eV. Even this highest estimated temperature, under typical conditions, is not sufficient for electronic excitation (the lowest excited state for RDX is calculated to be at 5.1 eV [32]). We propose the following to explain our observations for RDX in this work: since a 35 fs laser pulse provides a tremendous energy density and T-jump rate ($\approx 10^{14}$ K/s), a thermal and temperature "wave" could be generated, resulting in severe thermal stress on the samples. Under these conditions, thermally induced perturbations on the electronic structure could lead to reduction in bandgap energy—a similar process has been proposed for the mechanism of electronic excitation following a shock impact front through an RDX material containing dislocations [21]. Theoretical modeling of rapidly heated RDX will be performed in a future study to confirm this hypothesis.

It should be noted that the rate of thermal energy transfer from Au to the sample and the rate of heat transport within a sample depend on sample thicknesses, degree of homogeneity, and purity. Consequently, measurements of temperature from a surface of a thin film Au substrate could be significantly different from the real temperature obtained within a sample. Therefore, to determine the real temperature in a sample, a direct temperature measurement technique as described in Refs. [4] and [5] is needed, and will be applied to flash heated thin films in future work.

C. Transient Absorptions of Mixtures of RDX with OPE

In an effort to study the dependence of the thermal energy transfer rate on the sample homogeneity and purity, time-resolved

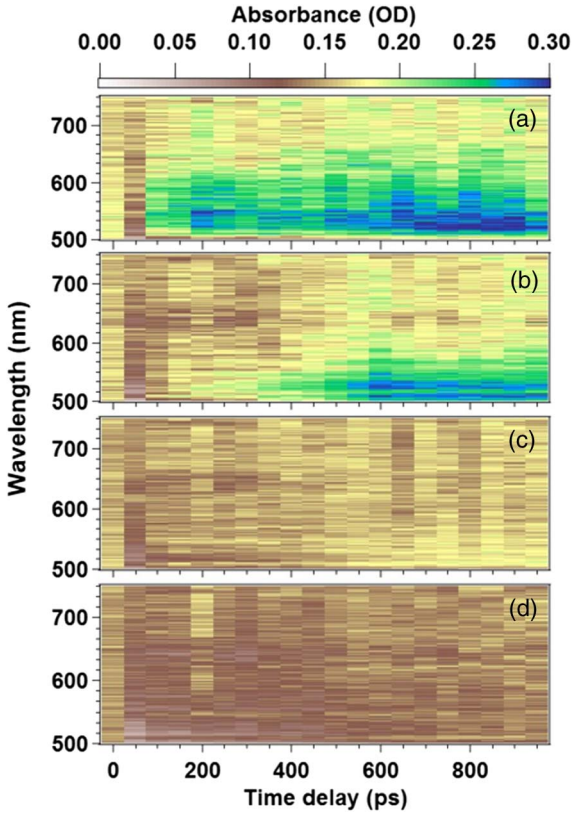

Fig. 7. 2D time-resolved transient absorption spectra of thin films RDX with (a) 1%, (b) 2.5%, (c) 5%, and (d) 10% OPE.

TA spectra of RDX with 1%, 2.5%, 5%, and 10% OPE were collected and are presented in Figs. 7(a)–7(d), respectively. In a general trend, the TA spectra of these samples become observable at longer delay times and have significantly lower

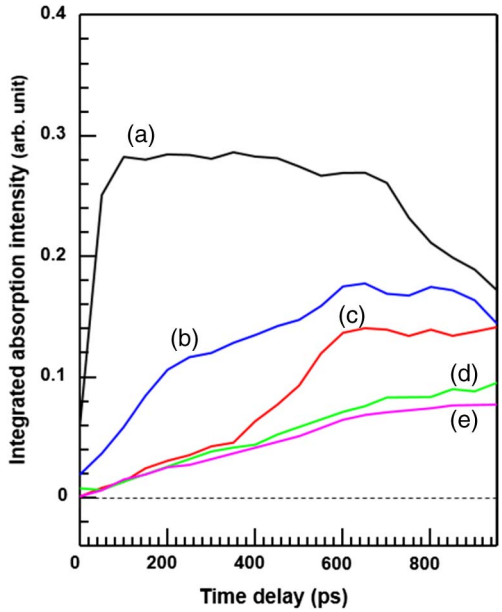

Fig. 8. Time-resolved profiles of transient absorption intensity of a (a) thin film RDX and films of RDX with (b) 1%, (c) 2.5%, (d) 5%, and (e) 10% OPE.

TA intensities as the amount of OPE in the RDX increases. The observations indicate that thermal energy transfer in RDX/OPE samples is less efficient compared to that in pure RDX. Since OPE has a significantly lower heat conductivity compared to that of pure RDX, the surrounding OPE dissipates (or absorbs) the heat, thus leading to a lower ΔT and heat transfer rate into the RDX crystal.

Figure 8 shows comparisons of ΔT and heat transfer rate of the RDX/OPE mixtures in terms of integrated transient absorption intensity as a function of time delay. The comparisons clearly indicate that ΔT decreases and occurs at a slower rate as the amount of OPE in RDX increases. While the time required for ΔT in RDX is 150 ps, it is found to be ~250 ps for 1% OPE and 620 ps for 2.5% of OPE in RDX. For RDX samples with 5% and 10% of OPE, the T-jump appears longer than 1 ns. The results are direct evidence that can be used to support and validate hypotheses for mechanisms of desensitizing RDX-based explosives with polymer binders [33], in which polymers are thought to absorb heat from local regions of initiation, including any hot spots, and dissipate heat away from the energetic material, preventing further decomposition of the adjacent molecules or particles (and thus the bulk material).

4. SUMMARY AND CONCLUSIONS

The response to ultrafast laser heating of RDX, OPE, and RDX/OPE mixtures was examined in terms of thermal energy transfer using TA spectroscopy in the range from 500 to 750 nm over a time window of 1000 ps. TA spectroscopy of RDX prior to decomposition exposed prominent features that are attributed to thermally induced perturbations on the electronic structure of RDX molecules being promoted to the excited state. This finding suggests that temperature participation in the shock-induced initiation of explosives occurs before the decomposition reactions, and that the excited states of energetic materials may play a role in explosive initiation.

No transient absorption was observed for OPE following flash heating, which was attributed to high heat dissipation in OPE, leading to lower heat transfer rates and, hence, lower T-jumps in the sample. Studies of the mixtures of RDX/OPE show that the TA intensity was significantly lower for the mixtures compared to that obtained for RDX and decreased as OPE content increased. These results confirm that OPE is a thermal barrier that blocks heat transferring into RDX.

Funding. Army Research Laboratory (ARL).

Acknowledgment. The authors wish to thank Dr. Rose Pesce-Rodriguez for providing the OPE sample used in this study. N. C. Dang was supported in part by appointment to the U.S. Army Research Laboratory Postdoctoral Fellowship Program administered by the Oak Ridge Associated Universities through a cooperative agreement with the U.S. Army Research Laboratory.

REFERENCES

1. A. N. Dremin, "Shock discontinuity zone effect: the main factor in the explosive decomposition detonation process," Philos. Trans. R. Soc. London A **339**, 355–364 (1992).
2. J. J. Gilman, "Chemical reactions at detonation fronts in solids," Philos. Mag. B **71**(6), 1057–1068 (1995).
3. D. D. Dlott, "New developments in the physical chemistry of shock compression," Annu. Rev. Phys. Chem. **62**, 575–597 (2011).
4. N. C. Dang, C. A. Bolme, D. S. Moore, and S. D. McGrane, "Femtosecond stimulated Raman scattering picosecond molecular thermometry in condensed phases," Phys. Rev. Lett. **107**, 043001 (2011).
5. N. C. Dang, C. A. Bolme, D. S. Moore, and S. D. McGrane, "Temperature measurements in condensed phases using non-resonant femtosecond stimulated Raman scattering," J. Raman Spectrosc. **44**, 433–439 (2013).
6. N. C. Dang, Z. A. Dreger, Y. M. Gupta, and D. E. Hook, "Time-resolved spectroscopic measurements of shock-wave induced decomposition in cyclotrimethylene trinitramine (RDX) crystals: anisotropic response," J. Phys. Chem. A **114**, 11560–11566 (2010).
7. Y. A. Gruzdkov, J. M. Winey, and Y. M. Gupta, "Spectroscopic study of shock-induced decomposition in ammonium perchlorate single crystals," J. Phys. Chem. A **112**, 3947–3952 (2008).
8. J. E. Patterson, A. S. Lagutchev, S. A. Hambir, W. Huang, H. Yu, and D. D. Dlott, "Time- and space-resolved studies of shock compression molecular dynamics," Shock Waves **14**, 391–402 (2005).
9. J. E. Patterson, Z. A. Dreger, M. S. Miao, and Y. M. Gupta, "Shock wave induced decomposition of RDX: time-resolved spectroscopy," J. Phys. Chem. A **112**, 7374–7382 (2008).
10. S. Root and Y. M. Gupta, "Chemical changes in liquid benzene multiply shock compressed to 25 GPa," J. Phys. Chem. A **113**, 1268–1277 (2009).
11. M. J. Winey and Y. M. Gupta, "Shock-induced chemical changes in neat nitromethane: use of time-resolved Raman spectroscopy," J. Phys. Chem. B **101**, 10733–10743 (1997).
12. Y. Yang, S. Wang, Z. Sun, and D. D. Dlott, "Propagation of shock-induced chemistry in nanoenergetic materials: the first micrometer," J. Appl. Phys. **95**, 3667–3676 (2004).
13. M. A. Zamkov, R. W. Conner, and D. D. Dlott, "Ultrafast chemistry of nanoenergetic materials studied by time-resolved infrared spectroscopy: aluminum nanoparticles in Teflon," J. Phys. Chem. C **111**, 10278–10284 (2007).
14. D. McGrane, D. S. Moore, and D. J. Funk, "Shock induced reaction observed via ultrafast infrared absorption in poly(vinyl nitrate) films," J. Phys. Chem. A **108**, 9342–9347 (2004).
15. N. C. Dang, C. A. Bolme, D. S. Moore, and S. D. McGrane, "Shock induced chemistry in liquids studied with ultrafast dynamic ellipsometry and visible transient absorption spectroscopy," J. Phys. Chem. A **116**, 10301–10309 (2012).
16. K. E. Brown, C. A. Bolme, D. S. Moore, and S. D. McGrane, "Ultrafast chemical reactions in shocked nitromethane probed with dynamic ellipsometry and transient absorption spectroscopy," J. Phys. Chem. A **118**, 2559–2567 (2014).
17. K. E. Brown, C. A. Bolme, D. S. Moore, and S. D. McGrane, "Ultrafast shock-induced chemistry in carbon disulfide probed with dynamic ellipsometry and transient absorption spectroscopy," J. Appl. Phys. **117**, 085903 (2015).
18. M. R. Armstrong, J. C. Crowhurst, S. Bastea, and J. M. Zaug, "Ultrafast observation of shocked states in a precompressed material," J. Appl. Phys. **108**, 023511 (2010).
19. D. D. Dlott and M. D. Fayer, "Shocked molecular solids: vibrational up pumping, defect hot spot formation, and the onset of chemistry," J. Chem. Phys. **92**, 3798–3812 (1990).
20. J. J. Gilman, "Mechanochemistry," Science **274**, 65 (1996).
21. M. M. Kuklja, B. P. Aduev, E. D. Aluker, V. I. Krasheninin, A. G. Krechetov, and A. Y. Mitrofanov, "Role of electronic excitations in explosive decomposition of solids," J. Appl. Phys. **89**, 4156–4166 (2001).
22. A. B. Kunz, M. M. Kuklja, T. R. Botcher, and T. P. Russell, "Initiation of chemistry in molecular solids by processes involving electronic excited states," Thermochim. Acta **384**, 279–284 (2002).
23. J. E. Field, "Hot spot ignition mechanisms for explosives," Acc. Chem. Res. **25**, 489–496 (1992).

24. M. J. Maurer and H. A. Thompson, "Non-Fourier effects at high heat flux," J. Heat Transfer **95**, 284–286 (1973).
25. A. M. Altshuler, "Detonation waves of transformations in energetic materials: an assessment of Soviet research," Report No. TRC-90-001 (Technical Research Corporation, 1990).
26. J. A. Carter, Z. H. Wang, H. Fujiwara, and D. D. Dlott, "Ultrafast excitation of molecular adsorbates on flash-heated gold surfaces," J. Phys. Chem. A **113**, 12105–12114 (2009).
27. C. M. Berg, A. Lagutchev, and D. D. Dlott, "Probing of molecular adsorbates on Au surfaces with large-amplitude temperature jumps," J. Appl. Phys. **113**, 183509 (2013).
28. T. Lou and J. R. Lloyd, "Non-equilibrium molecular dynamics study of thermal energy transport in Au-SAM–Au junctions," Int. J. Heat Mass Transfer **53**, 1–11 (2010).
29. R. A. Pesce-Rodriguez and S. M. Piraino, "Chemical and physical characterization of comp A-3 type II prills," Report No. ARL-TR-6498 (U.S. Army Research Laboratory, 2013).
30. J. D. Yeager, K. J. Ramos, R. A. Pesce-Rodriguez, and S. M. Piraino, "Microstructural effects of processing in the plastic-bonded explosive composition A-3," Mater. Chem. Phys. **139**, 305–313 (2013).
31. J. Hohlfeld, S.-S. Wellershoff, J. Güdde, U. Conrad, V. Jähnke, and E. Matthias, "Electron and lattice dynamics following optical excitation of metals," Chem. Phys. **251**, 237–258 (2000).
32. A. Bhattacharya and E. R. Bernstein, "Nonadiabatic decomposition of gas-phase RDX through conical intersections: an ONIOM-CASSCF study," J. Phys. Chem. A **115**, 4135–4147 (2011).
33. R. C. Bowers, J. B. Romans, and W. A. Zisman, "Mechanisms involved in impact sensitivity and desensitization of RDX," Ind. Eng. Chem. Prod. Res. Dev. **12**, 2–13 (1973).